Supplementary Information

Photon Cascade from a Single Crystal Phase Nanowire Quantum Dot

Maaike Bouwes Bavinck, Klaus D. Jöns, Michal Zieliński, Gilles Patriarche,

Jean - Christophe Harmand, Nika Akopian, and Val Zwiller

Supp. Information 1 – Polarization for optical transitions of Figure 1d).

Figure S1 shows the polarization for the transitions labeled X and XX in Figure 1d). We determine the polarization by performing Stokes measurements. We measure the spectrum in six different bases: the linear polarization along (z) and perpendicular to the nanowire, diagonal and anti-diagonal, and the left and right circular components. The analyzed data is shown in
Figure S1 together with the direction of the nanowire. We observe a strong linear component along the nanowire for both the X and XX transitions.

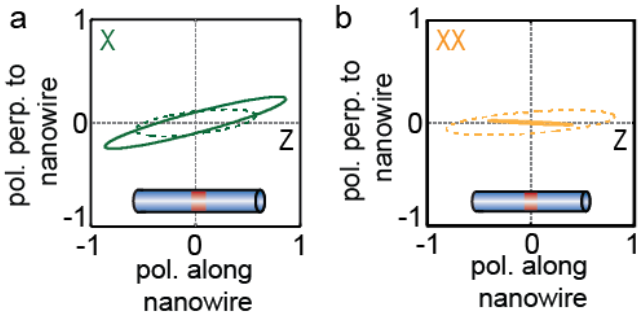

Figure S1. The polarization for the transition shown in Figure 1d) are strongly polarized along the nanowire for X (a) and XX (b).

Supp. Information 2 – Additional spectra

In Figure S2 we show additional spectra of crystal phase quantum dots in four different nanowires.

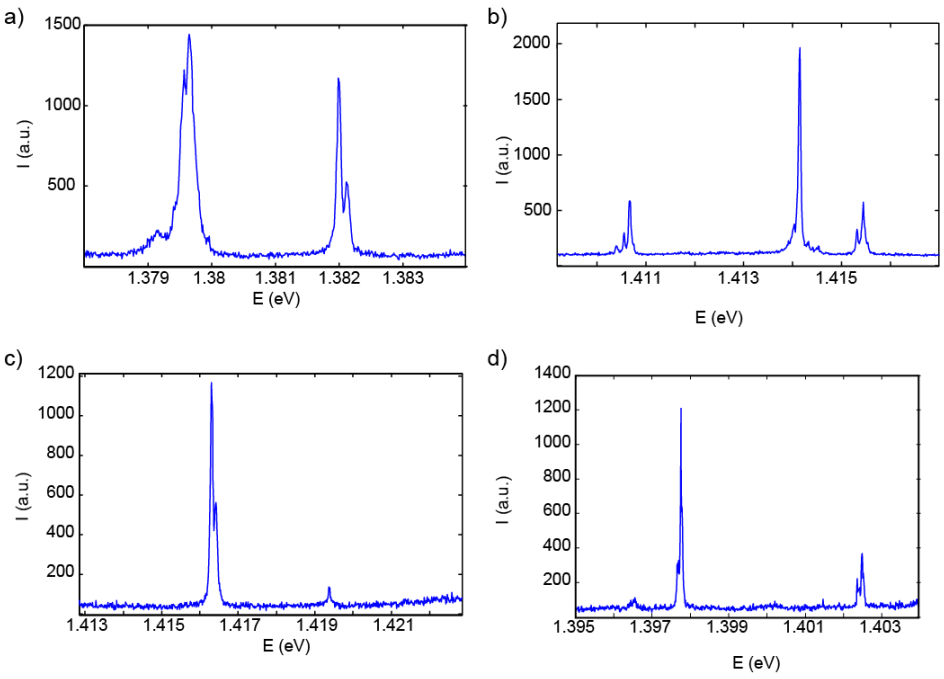

Figure S2. Four additional spectra from crystal phase quantum dots measured on different nanowires. All spectra show the double peak feature similar to the quantum dots measured in the main text and predicted by our calculations.

Supp. Information 3 - Theoretical Calculations - Methods

We use empirical tight-binding theory for the electron and hole states with an *sp3s** orbital model and nearest neighbors coupling. For the zinc blende InP section, we use Vogl et al.[1] tight-binding parameters augmented to account for spin-orbit effects. For the wurtzite InP section, we have additionally modified the parameters from Vogl et. al.[1] to account for the increased band-gap and the valence band offset between the wurtzite and zinc blende segments. We model the quantum dots by a zinc blende InP segment of height $(ZB)_n$, where n is number of (ABC) stacks, along the [111] direction embedded between two wurtzite InP segments along [0001] direction. The electronic structure calculation for different crystal polytypes is still an active field of research[2]. We fit our tight-binding parameters to reproduce the wurtzite band gap (1.474 eV), and the wurtzite-zinc blende valence band offset (64.6 meV) as has been recently reported by De and Pryor[2]. The zinc blende band gap is set to 1.41 eV. The spin-orbit splitting is assumed to be identical in the zinc blende and wurtzite crystal phases and is equal to 126 meV.

The crystal field splitting in wurtzite induces a relatively small splitting of A and B bulk hole bands. Unfortunately, this parameter is not reliably known, leading effectively to A-B splitting varying from 16 to over 70 meV[3,2], depending on the choice of the crystal field splitting parameter. Similarly, zinc blende/wurtzite lattice mismatch is reported in a wide range of values from 0.2% to over 1.0%[4,5]. With the zinc blende lattice constant being somewhat larger than that of wurtzite, lattice mismatch would in principle induce small tensile strain in the wurtzite region, that would act on the A-B splitting in opposite way to crystal field splitting effect. As neither strain parameters nor crystal field splitting are reliably know for wurtzite InP phase, in this work we decided to neglect both effects systematically. However, we checked that for different values of crystal field splitting and the inclusion of this effect, the excitonic emission energies changed well below 1 meV. Additionally, using zinc blende InP band deformation potentials, we estimate that strain at the interface between zinc blende and wurtzite would have effect on the energy spectra limited to several meV's.

Once the tight-binding Hamiltonian is established, we calculate the single particle spectra. We use the Hamiltonian matrix sparsity and calculate several lowest electron and hole states. The appearance of a free surface leads to the existence of spurious surface states due to dangling

bonds. We shift the dangling bond energies to shift the energies of surface-localized states away from the energies corresponding to the wurtzite/ zinc blende InP band gap region. We assume the wurtzite segments lengths to be equal to 30 nm (100 monolayers), resulting in a total domain height of more than 60 nm. This dimension is consistent with the experimentally observed density of zinc blende sections (15 segments/μm), i.e. ~60 nm per entire wurtzite-zinc blende-wurtzite system. The single particle computation is than followed by a configuration interaction method[3] for many-body states calculation and to obtain the excitonic optical (absorption) spectra. A calculation for the largest diameter system containing about 5 million atoms is the limit of what can be calculated with available computational resources.

Supp. Information 4 – Electron and hole states

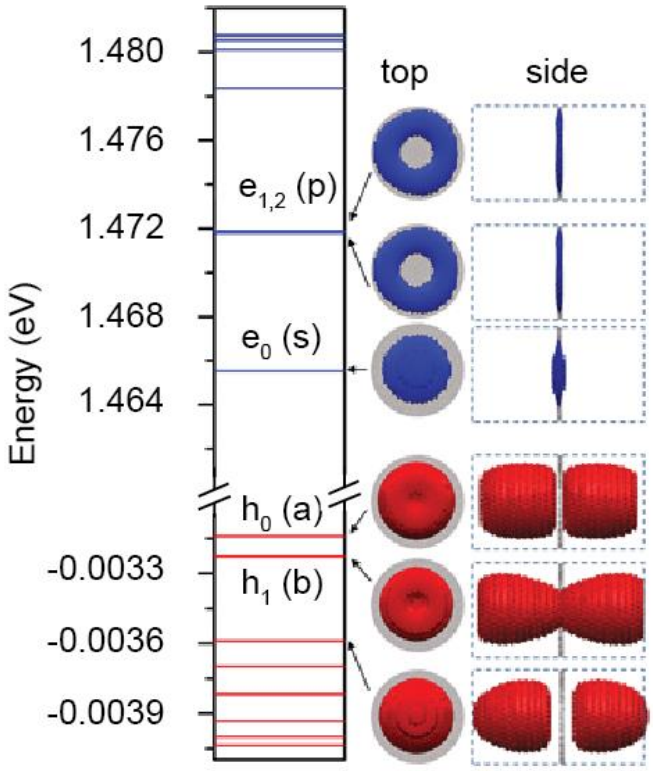

Figure S3. Single particle energies (left) and the corresponding charge densities for several lowest electron (up/blue) and hole (down/red) states in a crystal phase quantum dot system built from a single zinc blende section of height $(ZB)_1$

Figure S3 shows the single particle energies and the corresponding charge densities for several lowest electron and hole states in a crystal phase quantum dot system built form a single zinc blende sequence, $(ZB)_1$, embedded into a wurtzite nanowire of 32 nm diameter. The left isosurface plot (electron density of $3 \cdot 10^{-4}$ and hole $2 \cdot 10^{-5}$ densities) in the figure corresponds to a view along the nanowire growth axis and the plot on the right shows the isosurface along the nanowire. The single particle structure of the confined electron states in the zinc blende segment closely resembles that of self-assembled or nanowire quantum dots. The ground electron state is of s-like character, whereas the first and second excited electron states are of p-like character, with small (~0.1 meV) p-shell splitting due to the quantum dot symmetry (C_{3v}). The higher

electron states are delocalized over the nanowire. The spacing between the s- and p-electron states is 6.3 meV and is much smaller than in e.g. InAs/InP nanowire quantum dots. This is due to the shallow electron confining potential of the wurtzite – zinc blende conduction band offset (129 meV) and the reduced lateral confinement because of the relatively large nanowire diameter. The single particle hole states are very different from the electron states. They are delocalized over the wurtzite part of the nanowire and the energy spacing between subsequent hole states are small due to reduced confinement in wurtzite sections. The ground (h_0) and the first excited (h_1) hole states form a pair of closely energetically spaced states, separated only by 88 μeV. The first excited hole states is further separated by 360 μeV from the higher excited hole states.
The hole states localized in the left and right wurtzite sections of the nanowire are coupled via the zinc blende barrier to form an anti-bonding state (ground hole state) and a bonding state (excited hole state) delocalized over the entire system. The dipole moment between the ground hole state and ground electron state is about four orders of magnitude weaker than the dipole moment between the first excited hole state and the ground electron state.

With increasing nanowire diameter, the overall single particle properties remains unaltered, however, the inter-level energy differences are significantly reduced. For a nanowire with a diameter of 48 nm the spacing between s-like and p-like electron states is 3 meV and the p-shell splitting is only 25 μeV. The difference between h_0 and h_1 is 19 μeV, whereas h_2-h_1 spacing is only 63 μeV. The reduces inter-level spacing will lead to significant configuration mixing.

The single particle configuration is then followed by many-body (configuration interaction, exact diagonalization) calculation. Due to computational limits, in this calculation we include three lowest electron states (6 with spin), what effectively corresponds to accounting for electron and s- and p-shells. On the hole side we include 4 lowest (8 with spin) states. Therefore we account for 48 configurations to solve the single exciton problem, and 480 configurations for the biexciton.

Supp. Information 5 – Z and x/y polarization for different diameter and different crystal phase quantum dot configurations.

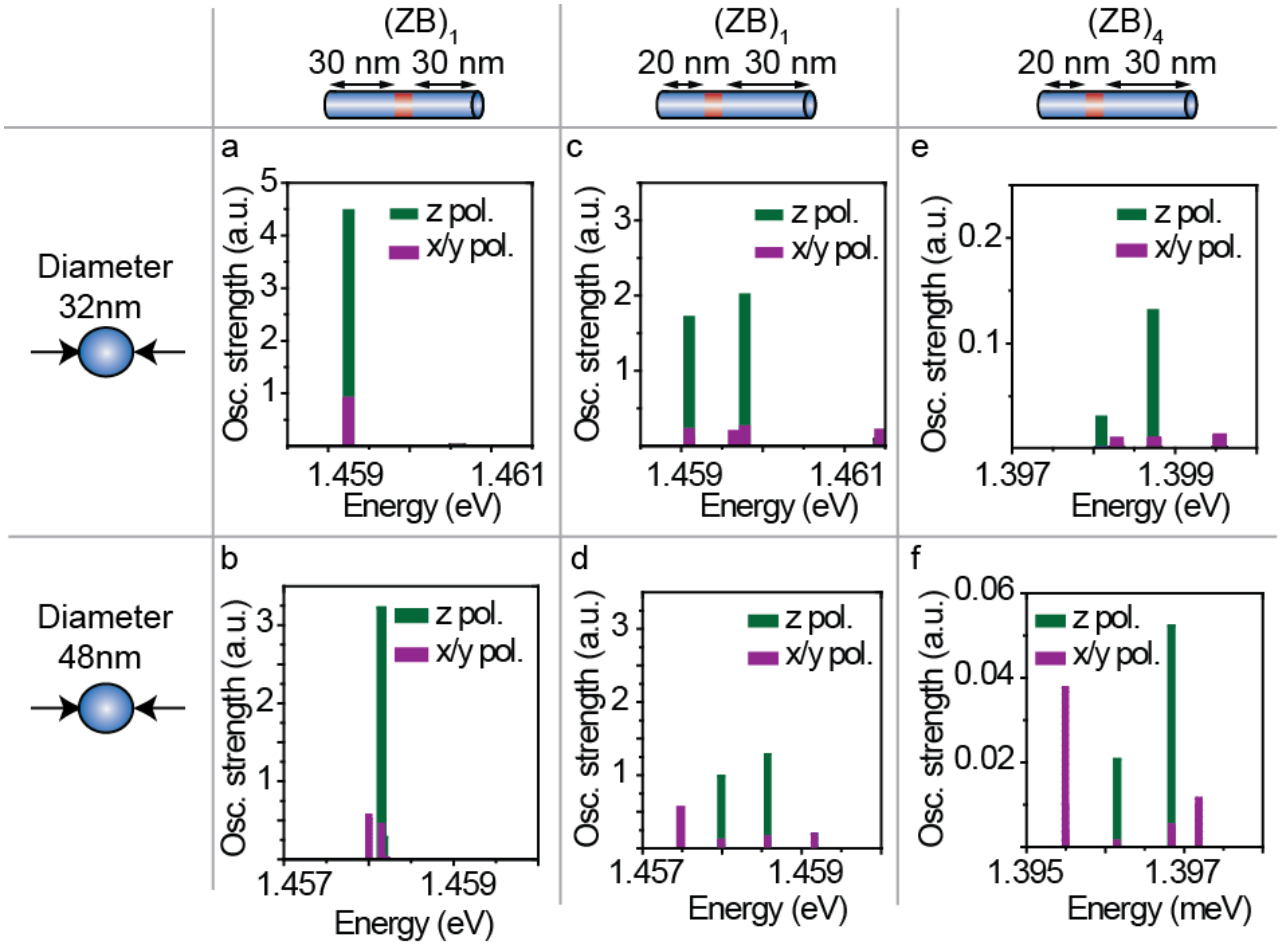

Figure S4. Calculations for different crystal phase quantum dot configurations. For two different diameters we show the results for a zinc blende section of size $(ZB)_1$ incorporated in a symmetric ((a) and (b)) and asymmetric wurtzite matrix ((c) and (d)). Figure (e) and (f) show a zinc blende section of $(ZB)_4$ in an asymmetric wurtzite matrix.

In Figure S4 we summarize our results of the calculations for different crystal phase quantum dot systems. We performed detailed calculations for two different nanowire diameters 32 nm and 48 nm. One can extract from the figures different trends. For a zinc blende section of $(ZB)_1$ in a symmetric matrix one observes a single peak for z-polarized light. When breaking the symmetry of the wurtzite matrix, the peak is split into two peaks. This is also the case for larger zinc blende structures ($(ZB)_4$), however, the overall oscillator strength is lower. For x/y-polarized lines, the intensity is weaker than the z-polarized transition, except for Figure S4f), where the z-polarized

and x/y-polarized lines are of the same strength. Also, we notice that the oscillator strength for all transitions decreases for increasing diameter.

Supp. Information 6 – Lifetime

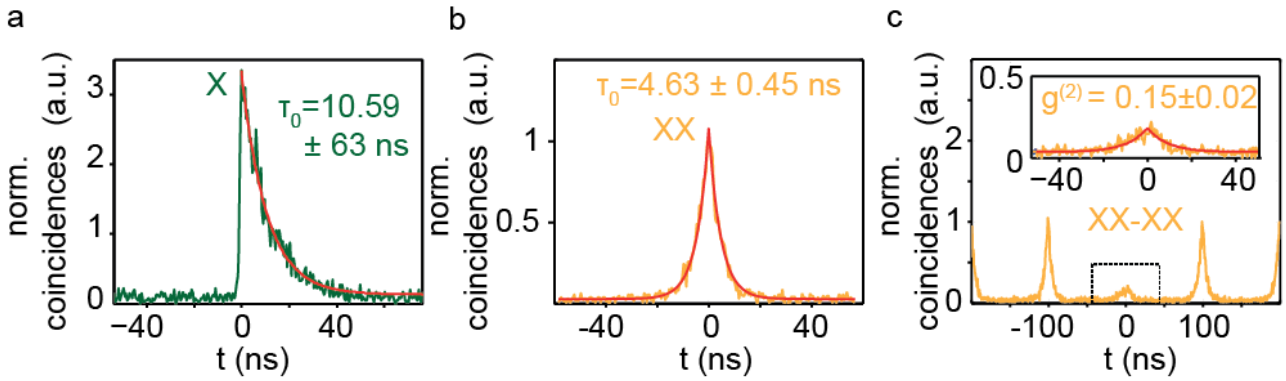

Figure S5. The measured and fitted lifetime for the (a) exciton and (b) biexciton. Figure (c) shows the fit to extract the g_2 value from the biexciton.

Figure S5 shows the fits that we used to extract the lifetimes and $g^{(2)}(0)$. To extract the lifetime of the exciton we use the cross-correlation measurements (Figure S5a)) and we use the auto-correlation measurement of the biexciton for the biexciton lifetime (Figure S5b)). We fit the data with a single exponential: $N(t) = A\left(1 - e^{\left|\frac{t-t_0}{\tau_0}\right|}\right)$, where A and t_0 are fitting parameters and τ_0 is the lifetime. For the exciton we extract a lifetime of 10.59 ± 0.63 ns and for the biexciton a lifetime of 4.63 ± 0.45 ns. We fit the antibunching peak of the biexciton (Figure S5c)) to extract a $g^{(2)}(0)$ of 0.15± 0.02. We observe a small dip at t = 0 ns indicating possible re-excitation of the quantum dot.

References

(1) Vogl, P., Hjalmarson, H. P. , & Dow, J.. *J. Phys. Chem. Solids* **1983**, *44*, 365.

(2) De, A. & Pryor, C. E.. *Phys. Rev. B* **2010**, *81*, 155210

(3) Zhang, L., Luo, J.-W., Zunger, A., Akopian, N., Zwiller, V., & Harmand, J.-C. *Nano Lett.* **2010**, *10*, 4055.

(4) Kriegner, D., Wintersberger, E., Kawaguchi, K., Wallentin, J., Borgström, M.T., & Stangl, J. Nanotechnology **2011**, *22*, 425704.

(5) Dacal, L. C. O. & Cantarero, A. Solid State Commun. **2011**, *151*, 781.

(6) Zielinski, M., Korkusinski, M., & Hawrylak, P. Phys. Rev. B **2010**, *81*, 085301.